CrossMark

ORIGINAL PAPER

Colloidal Stability and Toxicity of Gold Nanoparticles and Gold Chloride on *Chlamydomonas reinhardtii*

Renata Behra · Bettina Wagner · Linn Sgier · David Kistler

Abstract Here we have examined interactions of gold nanoparticles differing in primary particle size and coating with the green algae *Chlamydomonas reinhardtii* as function of the colloidal stability of the particles in the experimental media used for toxicity studies. Interactions of dissolved Au^{3+} ions with algae were also examined. Included endpoints were photosynthetic yield and algal growth. Morphological and structural effects were examined microscopically and by flow cytometry. The results indicate no significant toxicity of gold nanoparticles to *C. reinhardtii*. Analysis of published data suggests toxicity of gold nanoparticles on algal growth to relate rather to particular coatings than to the gold core.

Keywords Gold nanoparticles · Coatings · Colloidal stability · Toxicity · *Chlamydomonas reinhardtii*

1 Introduction

Nanoecotoxicology is the field of research that has emerged in response to the continuous growth and developments of nanotechnology and which deals with nanoparticles (NP) to identify and predict effects on organisms and ecosystems (Schirmer et al. 2013). So far, a major focus of research has been on quantifying the toxicity of diverse NP to various

R. Behra (✉) · B. Wagner · L. Sgier · D. Kistler
Department of Environmental Toxicology, Eawag, Swiss Federal Institute of Aquatic Science and Technology, Dübendorf, Switzerland
e-mail: renata.behra@eawag.ch

R. Behra
Institute of Biogeochemistry and Pollutant Dynamics, ETH-Zürich, Zurich, Switzerland

terrestrial and aquatic organisms. These studies suggest that properties that make NP of interest for various applications do not impinge on a particularly high toxicity to organisms. However, many fundamental mechanistic questions on uptake, distribution, accumulation, and effects of NP are unexplored in most organisms and need to be considered in order to support regulatory decisions based on a sound scientific knowledge.

Eukaryotic unicellular algae, being at the base of food webs in aquatic ecosystems and relevant to biogeochemical cycling of elements, serve as model organisms in ecotoxicological assessments to examine the effects of stressors on primary producers. So far, most studies concerned with the effects of NP on algae have reported on concentrations of various NP that inhibit growth in freshwater and marine algae (Farré et al. 2009; Handy et al. 2012; Kahru and Ivask 2013), while the mechanisms leading to observed inhibitory effects remain to be explored for any type of particles. Published studies indicate processes that affect stability and behavior of NP in experimental media, to also influence the toxicity outcome. For instance, dissolution of AgNP, ZnONP or CuONP contributes to toxicity by the formed metal ions (Bondarenko et al. 2013; Franklin et al. 2007; Ma et al. 2013; Miao et al. 2009; Navarro 2008b; Piccapietra et al. 2012a). In case of the less soluble CeO_2NP, toxicity to algae was attributed to indirect effects most probably occurring at cellular interfaces (Van Hoecke et al. 2009). Besides physical disturbance of cell walls and membranes, agglomerates of NP might induce effects through shading (Handy et al. 2012; Hartmann et al. 2013, 2009). While Ce^{3+} ions can be formed upon reduction of Ce^{4+} (Auffan et al. 2009), compared to other metal ions, Ce^{3+} displays a much lower toxicity (Peidong Tai et al. 2010; Röhder et al. 2014). Particle toxicity might be induced indirectly as in case of redox-active TiO_2NP also through generation of reactive oxygen species (Auffan et al. 2009). Altogether, occurrence of indirect effects makes conclusions on the direct contribution of particles to toxicity uncertain. Moreover, no studies have proved that NP toxicity to algae depends on their cellular internalization. Nevertheless, current knowledge appears to indicate particles composed of metals known to be highly toxic in their ionic form and prone to dissolve, to display higher toxicity than particles composed of metals that are not among the most toxic in their ionic form.

As a follow-up of our research, the aim of this study was to assess for interactions of gold nanoparticles (AuNP) differing in coating (carbonate and citrate), and gold(III) chloride with the green algae *Chlamydomonas reinhardtii* . AuNP are of interest since known to be chemically inert and resistant to oxidation. Based also on our previous studies indicating a rather unlikely cellular uptake of AgNP in *C. reinhardtii* (Piccapietra et al. 2012a; Schirmer et al. 2013), we hypothesized a moderate toxicity and a low physical interaction of particles with algae. Available information on the toxicity of AuNP to algae is limited to a few studies, each focussing on different algae species and different types of particles with regard to their coating or functionalization and colloidal stability (Garcia-Cambero et al. 2013; Hartmann et al. 2013; Perreault et al. 2012; Renault et al. 2008; Van Hoecke et al. 2013). While AuNP displaying a negative average charge appear to be rather innocuous, one same algae species shows to be sensitive to AuNP coated with a positive-charged coating, suggesting that effects might be caused rather by the coating (Renault et al. 2008; Van Hoecke et al. 2013).

Here we have examined AuNP differing in size and coating, and their interactions with *C. reinhardtii* as function of the colloidal stability of the particles in the experimental media used for toxicity studies. Since little is known on the toxicity of dissolved Au^{3+} ions to algae (Garcia-Cambero et al. 2013; Nam et al. 2014; Tai et al. 2010), we also examined effects of Au^{3+} ions. Examined endpoints were photosynthetic yield and algal growth. Moreover, morphological and structural effects were examined microscopically and by

flow cytometry (FC) during growth of algae. Experiments were also carried out with a cell wall-free mutant of *C. reinhardtii* in order to explore the influence of the cell wall on the toxicity outcome.

2 Materials and Methods

Carbonate-coated AuNP (AuNP$_{carb}$) were purchased from NanoSys GmbH (Wolfhalden, Switzerland), and citrate-coated AuNP (AuNP$_{cit}$, diameter 5 nm) from Nanocs^{TM} were provided as aqueous suspensions of 250 μM Au and 507.7 μM Au based on the gold mass for the AuNP$_{carb}$ and AuNP$_{cit}$, respectively. Carbonate and citrate coatings maintain AuNP in suspension by avoiding aggregation. However, two batches of AuNP$_{carb}$ were used since the original suspension of AuNP$_{carb}$ (batch 1) showed a change in color (from red to dark purple) and some visible black aggregates after about 1 year of storage. The original AuNP suspensions were kept in the dark. Gold chloride (NaAuCl$_4$·2H$_2$O) was provided by Sigma-Aldrich. All solutions were prepared using deionized nanopure water (16–18 MΩ cm^{-1}; Barnstead Nanopure Skan AG, Basel-Allschwil, Switzerland).

2.1 Particle Characterization

Particles from stock suspensions were visually examined using transmission electron microscopes (TEM, CM30, FEI, and HD2700Cs, Hitachi). The microscopes were operated at 300 kV (CM30) and 200 kV (HD2700Cs). Images were recorded in bright-field mode (CM30) and in scanning mode using a high-angle annular dark-field detector (HD2700Cs).

For colloidal stability experiments, selected experimental concentrations of AuNP$_{carb}$ and AuNP$_{cit}$ were prepared using 5 mM MOPS buffer (3-morpholine propanesulfonic acid) pH 7.5, and the algal inorganic growth medium Talaquil (Le Faucheur et al. 2005). Particles were characterized for average size and Zeta potential by dynamic light scattering (DLS) using a Zeta Sizer (Nano ZS, Malvern Instruments) equipped with a 633-nm (He–Ne) laser. For the measurements, the dispersant was set to water and automatic settings were used, including a fixed scattering angle of 173 °C, automatic measurement duration, attenuation, and optimum measurement position. For Zeta potential measurements, automatic attenuation, and voltage, a minimum of 10 runs, and a maximum of 30 runs were selected. Three measurements were taken per sample, and the autocorrelation function was analyzed using the cumulant analysis algorithm, resulting in a mean size (*z*-average) and a standard deviation (SD) (polydispersity index, PDI). Data sets with a PDI above 0.7 were not taken into account. The stability of AuNP in natural water was also examined by exposing AuNP to 0.22 μm filtered Chriesbach water under constant gentle stirring, following Piccapietra et al. (2012b). According to chemical analysis, 0.22 μm filtered Chriesbach water contained 3.72 mg/L, DOC had an ionic strength of 8.05 mM and a pH of 7.8. Average size and Zeta potential were measured after 1, 2, and 24 h.

2.2 Metal Measurements

For total gold concentration (isotope ^{197}Au), samples were acidified using aqua regia (1:3 nitric to hydrochloric supra pure acid) to achieve 6.2 % final acid concentration. Prior to measurements by ICP-MS (Element 2 High Resolution Sector Field ICP-MS; Thermo-Fischer, Switzerland), samples were digested in a high-performance microwave (ultraclave, MLS, Leutkirch, Germany). Reliability of the measurements was controlled using specific

water references (ref M105A20, IFA Systems). Gold standard (Trace CERT®Ultra) was used for calibration. Compared to nominal concentrations, the measured Au concentration was between 110 and 116 % in AuNP$_{carb}$ suspensions of batch 1 and 2, 131 % in the NaAuCl$_4$ solution, and only 13 % in the AuNP$_{cit}$ suspensions.

2.3 Algal Cultures

The wild type of the unicellular freshwater alga *C. reinhardtii* (strain CC 125) and the cell wall-free mutant (strain CC 400) were obtained from the Chlamydomonas Genetics Centre (Durham, USA). Algae in the inorganic growth medium Talaquil (pH 7.5) were grown in glass Erlenmeyers under controlled conditions (23 °C, 90 rpm, 120 μE m^{-2} s^{-1}) using a High Technology Infors shaker (Infors, Bottmingen, Switzerland) as described previously by Scheidegger et al. (2011). Due to a different sensitivity to mechanical stress, two different centrifugation protocols were applied for inoculation and subculturing (10 min, 1500 rpm for the mutant and 10 min, 3000 rpm for the wild type).

2.4 Exposure of algae to Au(III) and AuNP, and endpoint measurements

For toxicity experiments, exponentially growing algae were suspended in the experimental media to obtain a final density of 2×10^5 cells mL^{-1}. Effects on algal photosynthetic yield were determined by short-term experiments in 10 mM MOPS (pH 7.5) in case of AuNP, and with the addition of NaCl (final concentration 10 mM) in case of NaAuCl$_4$ exposures. In the simple buffer medium MOPS which is used in our experiments to avoid metal ion complexation (Schirmer et al. 2013; Tai et al. 2010), algae maintain their photosynthetic activity up to 4 h (Navarro 2008b). Photosynthetic yield was not affected by NaCl. Toxicity of AuNP and NaAuCl$_4$ to photosynthetic yield was assessed by concentration–response experiments, exposing algae to increasing concentrations of AuNP$_{carb}$ (batch 1) (from 1 to 50 μM) and to NaAuCl$_4$ (from 1 to 120 μM) for one and two h.

Photosynthetic yield of photosystem II which reflects the efficiency of photochemical energy conversion was measured fluorometrically using a PHYTO-PAM (Heinz Walz GmbH) according to Navarro (2008b). The yield was calculated as $(F_m - F_t)/F_m$, where F_t is the fluorescence measured immediately after a saturating light pulse and F_m corresponds to the basal fluorescence (Schreiber 1998). Photosynthetic yield, expressed as % of control, was plotted as a function of the nominal AuNP or Au(III) concentration. In case of Au(III), data points were fitted to a four-parameter logistic curve using Sigma Plot 9.0 (SPSS Inc., USA), to obtain the corresponding EC$_{50}$ values as described by Navarro (2008b).

Effects of AuNP on algal growth were performed by exposing both algal strains in Talaquil to 10 μM AuNP$_{carb}$ (batch 1 and 2) up to 48 h. The cell number was measured at various times using an electronic particle counter (Z2 Coulter Counter, Beckman Coulter, Fullerton, CA, USA; Casy Model TT, Roche, Germany).

All errors are expressed as SD except for EC$_{50}$ results which are expressed as standard errors (SE).

Cell morphology during growth of algae exposed to 10 μM AuNP$_{carb}$ was examined by light microscopy using a Leica DMI 6000B epifluorescence microscope (Leica Microsystems, Wetzlar, Germany). Granularity of cells was analyzed by FC. For FC measurements, cells were counted and fluorescence of the sample was measured with a GalliosTM flow cytometer (Model; 3L 10C, 561READY) (Beckman Coulter Inc., Nyon, Switzerland). The instrument is equipped with four solid-state lasers, which provide excitation wavelength at 488 nm (22 mW), 561 nm (21.5 mW), 638 nm (25 mW), and

405 nm (40 mW). The trigger was set on forward scattered light (FSC), as this provides optimal separation between algae cells and background signals. In order to examine the granularity of algal cells, the sideward scatter (SSC) and green fluorescence (FL4) were measured upon excitation with the 488-nm laser. Optimal separation of differences in the relative SSC intensity compared to control samples was obtained by specific instrument gain settings. The cytometer was operated by continuous pressure applied to the sample tube based on user selected flow rate (high, approximately 60 μL/min). Kaluza for Gallios acquisition software 1.0 was used for data acquisition, and Kaluza Analysis software 1.3 was used for statistical analysis.

3 Results

3.1 AuNP Stability in MOPS, Talaquil, and Chriesbach Water

TEM analysis of the $AuNP_{carb}$ (batch 1) from the stock solution showed particles to be monodispersed with sizes of about 10–20 nm (Fig. 1). Physicochemical characteristics of the examined $AuNP_{carb}$ are shown in Table 1 (batch 1) and Table S1 (batch 2). DLS measurements of the stock solutions (each 250 μM $AuNP_{carb}$) showed particles to display different sizes (average diameter 18.5 and 55 nm, for batch 1 and 2, respectively). When diluted in 10 mM MOPS (pH 7.5), the medium used for photosynthesis experiments, $AuNP_{carb}$ (batch 1) showed particles in 100 μM suspensions to display an average diameter of 22 nm, which increased up to 100 nm in 5 μM $AuNP_{carb}$ suspensions (Table 1). $AuNP_{carb}$ (batch 2) suspensions maintained a similar average size upon dilution in MOPS (Table S1). Upon dilution in MOPS, particles from both batches displayed less negative Zeta potential values compared to the respective stock suspensions (Tables 1, S1). Analysis of $AuNP_{carb}$ (batch 2) suspensions in Talaquil, the medium used in growth inhibition experiments, and in Chriesbach water (pH 7.8) showed particles to have comparable average sizes as particles in MOPS buffer 1 h after dilution (Table 3). Similar sizes were measured over time (Table S2). Measurements of Zeta potential of $AuNP_{car}$ showed values to be comparable in suspensions of MOPS, Talaquil, and Chriesbach water that generally shifted to less negative values in all media at the lowest particle concentration of 10 μM $AuNP_{car}$ (Tables 1, 2, 3, S2).

TEM analysis of the $AuNP_{cit}$ from the stock solution (507 μM) imaged particles with a diameter size in the range of 2–5 nm (Fig. 1). In MOPS, particles increasingly agglomerated with increasing dilution to sizes up to 464 nm after 1 and 2 h (Table 2). In 10 μM $AuNP_{cit}$ suspensions, particles agglomerated up to 480 nm in Talaquil and less in Chriesbach water after 1 and 2 h (Table S3). However, $AuNP_{cit}$ agglomerated in Chriesbach water to a size of 640 nm after 24 h. At the lowest particle concentration, the Zeta potential of the $AuNP_{cit}$ shifted to less negative values from about -30 mV to about -8 mV in all media.

3.2 Photosynthetic Yield, Growth, and Cell Morphology

Effects on photosynthetic yield were assessed in MOPS. After 1 and 2 h exposure, $AuNP_{car}$ (batch 1) did not affect the photosynthetic yield neither in the wild type nor in the cell wall-free mutant at concentrations up to 50 μM (Figure S1). Similarly, $AuNP_{cit}$ did not alter the photosynthetic yield in the wild type. Growth experiments in Talaquil at a concentration of 10 μM $AuNP_{car}$ (batch 2) did not evidence any inhibitory effects in both strains (Figure
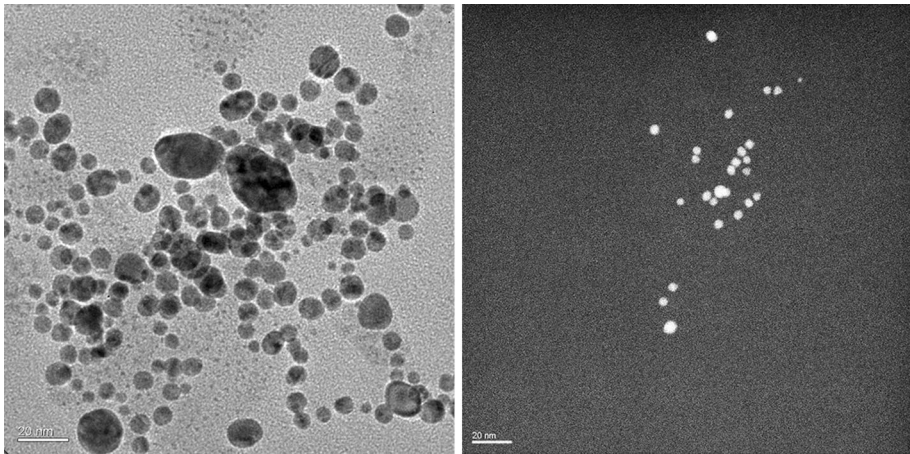
Fig. 1 TEM images showing AuNP$_{carb}$ (batch 1, *left* bright-field image) and the AuNP$_{Cit}$ (*right* high-angle annular dark-field image)

Table 1 Mean particle diameter, polydispersity index (PDI), and Zeta potential (ZP) of AuNP$_{carb}$ (batch 1) by DLS, 1 h after dilution of the stock solution in 10 mM MOPS, pH 7.5. The SD of three analytical replicates is indicated

AuNP$_{carb}$ (μM)	Size (nm)	SD	PDI	ZP (mV)	SD
5	101	16.1	0.7	−14.4	1.2
10	41	10.0	0.7	−17.6	3.3
50	27	0.3	0.6	−27.2	3.9
100	22	0.3	0.4	−30.3	1.4
250	18	1.1	0.4	−33.0	2.2

Table 2 Mean particle diameter, polydispersity index (PDI), and Zeta potential (ZP) of AuNP$_{cit}$ measured by DLS 1 and 2 h after dilution of the stock solution in 10 mM MOPS, pH 7.5. The SD of three analytical replicates is indicated

AuNP$_{cit}$ (μM)	Time (h)	Size (nm)	SD	PDI	ZP (mV)	SD
10	1	464	51	0.5	−11.1	1.3
10	2	422	68	0.6	−8.3	0.3
50	1	150	13	0.4	−29.1	1.7
50	2	181	13	0.4	−28.3	4.4
100	1	200	12	0.4	−30.1	0.8
100	2	213	10	0.4	−27.6	0.4

S2). Light microscopic analysis during growth experiments was not indicative of any morphological effects (Fig. 2). Examinations of the SSA by FC indicated the granularity of algal cells exposed to 10 μM AuNP$_{carb}$ to be comparable to that of control algae after 24 h exposure (Fig. 3).

NaAuCl$_4$ decreased the photosynthetic yield in both algal strains in a time- and concentration-dependent manner (Fig. 4). After 2 h exposure, calculated effective

Table 3 Mean particle diameter and Zeta potential (ZP) of AuNP$_{carb}$ (batch 2) measured by DLS, 1 h after dilution of the stock solution in 10 mM MOPS, pH 7.5, Talaquil, and Chriesbach water. The SD of three analytical replicates is indicated

| AuNP	MOPS				Talaquil				Chriesbach water			
	Size (nm)	SD	ZP (mV)	SD	Size (nm)	SD	ZP (mV)	SD	Size (nm)	SD	ZP (mV)	SD
10 μM AuNP$_{Carb}$	74	17	−12.0	1.7	74	3	−17.5	2.1	117	49	−13.5	1.2
50 μM AuNP$_{Carb}$	76	5	−21.5	0.6	72	6	−20.1	2.7	70	13	−12.9	1.1
100 μM AuNP$_{Carb}$	63	4	−26.5	1.7	68	7	−21.3	1.6	69	1	−16.2	1.8
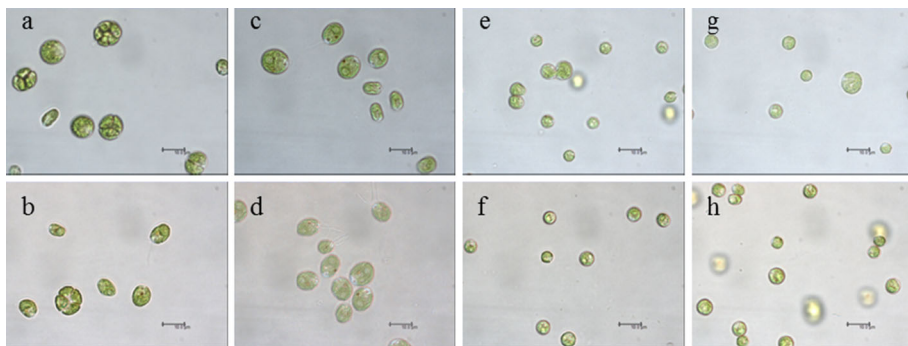
Fig. 2 Light microscopic images of the wild type (**a–d**) and the cell wall-free mutant (**e–h**) during growth of control (**a, b, e, f**) cells and cells exposed to 10 μM AuNP$_{carb}$ (**c, d, g, h**). Cells were visualized at times 15 h (*upper row*) and 22 h (*lower row*). The *scale bar* corresponds to 10 μm

concentrations decreasing the photosynthetic yield by 50 % (EC$_{50}$) were 8.6 ± 0.7 μM for the wild type and 8.8 ± 1.6 μM for the mutant (Table 4). The sideward scatter and the green fluorescence were comparable between control and NaAuCl$_4$-exposed algae (not shown).

4 Discussion

Interactions of NP with organisms show to be influenced by factors that alter their physicochemical characteristics as their size, surface charge, agglomeration state, shape, and chemical reactivity. Besides pH and ionic strength, components of experimental media used in ecotoxicity studies will also influence the physical and chemical properties of particles. Moreover, components secreted by organisms during toxicity studies will interact with NP eventually influencing their stability (Behra et al. 2013; Navarro et al. 2008a; Schirmer et al. 2013). Examination of the stability of the AuNP in experimental media used in this study indicated dynamic changes of the average size of the particles. TEM analysis of the original stock solutions evidenced an average size of 10–20 nm in case of the AuNP$_{car}$, and 2–5 nm for the AuNP$_{cit}$. In the simple system MOPS (10 mM MOPS, pH 7.5) that was originally designed as to maintain colloidal stability of AgNP coated with carbonate (Navarro 2008b; Piccapietra et al. 2012b), the colloidal stability of the AuNP
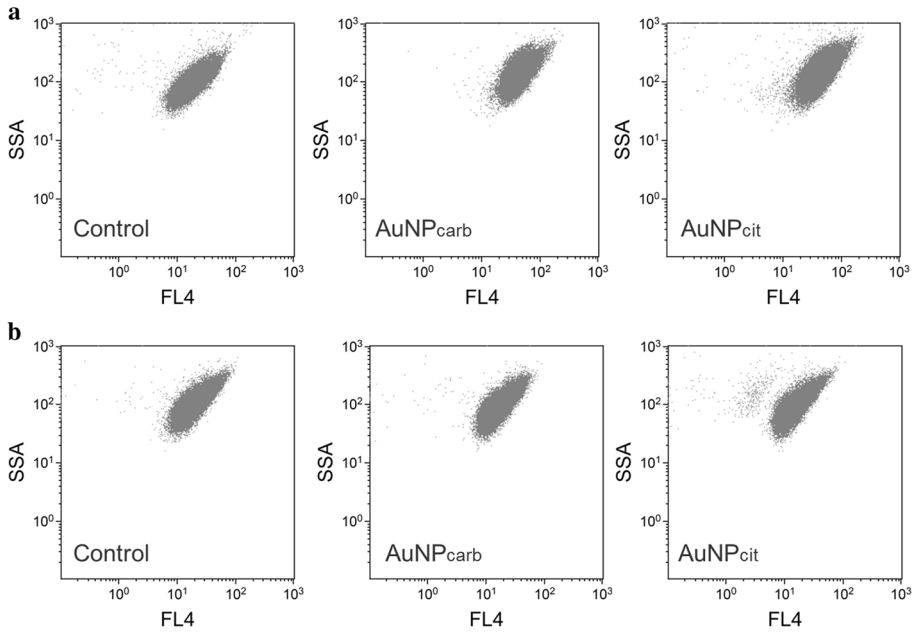
Fig. 3 Flow cytometry analysis of *C. reinhardtii* displaying the sideward scatter area (SSA) versus the green fluorescence (FL4) of the cells. Cells were analyzed after 24 h exposure of the wild type (**a**) and the cell wall-free mutant (**b**) to 10 μM AuNP$_{carb}$ (batch 2) and AuNP$_{cit}$ in Talaquil
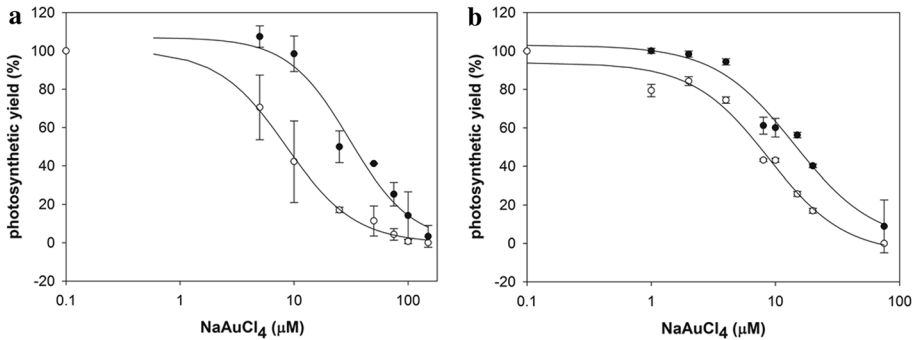
Fig. 4 Effect of NaAuCl$_4$ on photosynthetic yield in the wild type (**a**) and the cell wall-free mutant (**b**) of *C. reinhardtii* upon exposure for 1 (*open and filled circle*) and 2 (*filled and open circle*) h, as percentage of the corresponding control. The SD of 3 independent experiments is indicated

was apparently primarily controlled by the type and stability of their coating. Stability comparisons of MOPS suspensions at similar concentrations of gold showed a higher agglomeration of the smaller AuNP$_{cit}$ particles. In general, measured average Zeta potentials of AuNP$_{carb}$ and AuNP$_{cit}$ suspensions shifted to less negative values upon dilution. In case of the AuNP$_{carb}$, the Zeta potential linearly correlated with the degree of

Table 4 EC_{50} values of dissolved Au(III) determined after 1 and 2 h exposure of the wild type and the mutant of *C. reinhardtii*

	EC_{50} 1 h (µM)	EC_{50} 2 h (µM)
Wild type	30.7 ± 9.6	8.6 ± 0.7
Mutant	14.1 ± 3.4	8.8 ± 1.6

SD was calculated based on 3–5 independent experiments

agglomeration for the highest tested concentrations (Figure S1). The flattening of the curve at the lowest $AuNP_{carb}$ concentration might indicate some loss of the coating from the surface of particles in more diluted suspensions. Similar findings were reported for carbonate-coated silver NP in MOPS and were interpreted as the carbonate coating being subjected to a new equilibrium following dilution (Piccapietra et al. 2012b). Considering the presence of MOPS, we cannot exclude its contribution to the Zeta potential of the particles which appears to be similar at the lowest tested concentrations in both, $AuNP_{car}$ and $AuNP_{cit}$ supensions. In a comprehensive experimental and theoretical study with ZnONP, the coverage of the particle surface was clearly shown to determine the Zeta potential and thus the colloidal stability of the particles (Segets et al. 2011).

Examination of $AuNP_{car}$ and $AuNP_{cit}$ in the algal growth medium Talaquil as well as in Chriesbach water over time further indicated the presence of larger agglomerates in 10 µM suspensions that increased in case of the $AuNP_{cit}$ to sizes up to 639 nm after 24 h (Tables S2, S3). Compared to MOPS suspensions, increased agglomeration in these more complex media apparently results from interactions that occur between the surface of particles and media components and at higher ionic strength (Piccapietra et al. 2012b). Titration of CeO_2NP with inorganic components of Talaquil showed different effects on their charge and colloidal stability (Röhder et al. 2014). Time-dependent agglomeration and sedimentation of agglomerates of AuNP coated with starch and glucose in the inorganic OECD algal growth medium were observed previously by Hartmann et al. (2013) and were supposed to result from degradation of the coating. However, colloidal stability of AuNP strongly depends on the selected coating and its stability which strongly depends on the synthesis method (Chanana and Liz-Marzan 2012; Segets et al. 2011). From an eco-toxicological perspective, the time- and concentration-dependent changes of colloidal stability are challenging for disentangling direct particle effects from effects caused indirectly as through shading of algae, or the those caused by the coatings (Handy et al. 2012; Hartmann et al. 2009, Hartmann et al. 2013). While adequate control experiments allow tracking causes of assessed effects, relating uptake and effects to properties of NP is more complex task and often requires adaptation of experimental media to avoid major changes of colloidal stability during toxicity experiments (Sigg et al. 2014).

In our study with *C. reinhardtii*, we initially intended to examine how particle size influences interactions of AuNP with algae. AuNP are considered to be inert down to sizes of about 5 nm but display higher chemical reactivity and toxicity when diameters are below ~ 3 nm (Tsoli et al. 2005). Though TEM analysis of the $AuNP_{cit}$ from the original stock solution indicated an average particle size of 2–5 nm, particles formed agglomerates of ~ 200 nm in all media even at the highest tested concentration. Nevertheless, our experiments did not evidence any effect of AuNP on the examined endpoints. Thus, no effect was detectable on the photosynthetic yield in both strains exposed to concentrations up to 50 µM $AuNP_{carb}$ and $AuNP_{cit}$ (Figure S2) in MOPS, where particles displayed

average diameters >27 and >181 nm, respectively (Tables 1, 2). Also the growth of both strains was not inhibited at the examined $AuNP_{carb}$ concentration of 10 μM (Figure S3). Together these results indicate no significant toxicity of AuNP to *C. reinhardtii*. Among the few published studies on AuNP toxicity to algae (Hartmann et al. 2013; Renault et al. 2008; Segets et al. 2011; Van Hoecke et al. 2013) which have examined particles differing in coating, size, and colloidal stability, most report on a moderate toxicity on algal growth with effective concentrations in the mg/L Au range. However, higher toxicity on the growth of *Scenedesmus subspicatus* was reported in case of positively charged amine-coated AuNP (Renault et al. 2008). On the other hand, *Pseudokircheriella subcapitata*, though tested at a lower density, was less sensitive toward uncharged and negative-charged polymer-coated AuNP (Van Hoecke et al. 2013), suggesting modulating effects of the positive-charged amine group on algal toxicity (Van Hoecke et al. 2013). Interestingly, in the studies reporting on toxicity of AuNP to algae growth, TEM analysis did not evidence particle internalization in exposed cells (Hartmann et al. 2013; Renault et al. 2008; Segets et al. 2011; Van Hoecke et al. 2013), suggesting that particle uptake in cells is not a prerequisite for toxicity. As examined by FC and light microscopy, we did not detect any effects on the granularity or morphology of *C. reinhardtii* upon short- and long-term exposure to $AuNP_{carb}$ indicating a low level of particle–cells interactions, which was expected considering that algae display a negative surface charge. Similarly, little sorption to algae was reported for other negative-charged AuNP (Garcia-Cambero et al. 2013; Hartmann et al. 2013; Van Hoecke et al. 2013). On the other hand, AuNP stabilized with a positive-charged amine group were imaged to be attached to the cell surface and within its cellulose layer of the cell wall of *Scenedesmus subspicatus* (Renault et al. 2008). Yet, the question how AuNP induce toxicity to algal growth remains to be examined.

Toxicity of metal-based NP on algae seems to be controlled by their chemical stability. In case of more soluble metal-based NP, metal ions present or formed in NP suspensions of AgNP, CuONP, and ZnONP have been identified as a major cause of toxicity to algae (Bondarenko et al. 2013; Franklin et al. 2007; Ma et al. 2013; Miao et al. 2009; Navarro 2008b; Piccapietra et al. 2012a; Quigg et al. 2013). On the other hand, metallic NP displaying redox activity might induce toxicity upon formation of reactive oxygen that reacts with biomolecules leading to oxidative stress (Auffan et al. 2009; Behra et al. 2013; Tai et al. 2010). Moreover, elevated ROS formation might be induced by very low concentrations of dissolved metal ions as previously shown in *C. reinhardtii* (Szivak et al. 2009). In case of AuNP, neither dissolution nor abiotic formation of reactive oxygen species is expected considering the inertness of gold to react with oxygen (Cotton 1988). Moreover, gold ions are extremely unstable in aqueous solutions and are generally considered to be biologically inert. However, the possibility that physical interactions and disturbance of cell walls initiate oxidative stress responses cannot be excluded.

Au(III) provoked concentration- and time-dependent effects on the photosynthetic yield of *C. reinhardtii* (Fig. 4) that were moderate with EC_{50} in the low μM range after 2 h exposure (Table 4). The comparable EC_{50} determined for the wild type and the mutant indicate a minor role of the cell wall in Au^{3+} ion sorption. Previous demonstration that the cell wall indirectly protects *C. reinhardtii* from metal toxicity (Macfie et al. 1994) has been shown in case of silver to result from modulation of the uptake kinetics of Ag^+ ions, which is faster and higher in the cell wall-free mutant (Piccapietra et al. 2012a). Consequently, when effective concentrations are based on measured intracellular concentrations of Ag, sensitivity of photosynthesis is similar in both strains. Compared to inhibitory values obtained under similar experimental conditions, Au^{3+} toxicity to photosynthetic yield is similar to that of Ce^{3+} ions (Röhder et al. 2014) while Ag^+ ions are with EC_{50} of 195 nM

much more toxic (Navarro 2008b). Silver ions are taken up and accumulate fast in *C. reinhardtii* where they induce a series of molecular responses (Fortin and Campbell 2000; Leclerc and Wilkinson 2014; Piccapietra et al. 2012a; Pillai et al. 2014). So far, examination of mechanisms underlying uptake, accumulation, and toxicity of trivalent ions to algae is limited to few studies (Cremazy et al. 2013a; Cremazy et al. 2013b; Röhder et al. 2014).

References

Auffan M, Rose J, Wiesner M, Bottero JY (2009) Chemical stability of metallic nanoparticles: a parameter controlling their potential cellular toxicity in vitro. Environ Pol 157:1127–1133

Behra R, Sigg L, Clift MJD, Herzog F, Minghetti M, Johnston B, Petri-Fink A, Rothen-Rutishauser B (2013) Bioavailability of silver nanoparticles and ions: from a chemical and biochemical perspective. J R Soc Interface 10:1–15. doi:10.1098/rsif.2013.0396

Bondarenko O, Juganson K, Ivask A, Kasemets K, Mortimer M, Kahru A (2013) Toxicity of Ag, CuO and ZnO nanoparticles to selected environmentally relevant test organisms and mammalian cells in vitro: a critical review. Arch Toxicol 87:1181–1200. doi:10.1007/s00204-013-1079-4

Chanana M, Liz-Marzan LM (2012) Coating matters: the influence of coating materials on the optical properties of gold nanoparticles. Nanophotonics 1:199–220. doi:10.1515/nanoph-2012-0008

Cotton FA (1988) Advanced inorganic chemistry. Wiley, New York

Cremazy A, Campbell PGC, Fortin C (2013a) The biotic ligand model can successfully predict the uptake of a trivalent ion by a unicellular alga below pH 6.50 but not above: possible role of hydroxo-species. Environ Sci Technol 47:2408–2415. doi:10.1021/es3038388

Cremazy A, Levy JL, Campbell PGC, Fortin C (2013b) Uptake and subcellular partitioning of trivalent metals in a green alga: comparison between Al and Sc. Biometals 26:989–1001. doi:10.1007/s10534-013-9675-6

Farré M, Gajda-Schrantz K, Kantiani L, Barcelo D (2009) Ecotoxicity and analysis of nanomaterials in the aquatic environment. Anal Bioanal Chem 393:81–95. doi:10.1007/s00216-008-2458-2471

Fortin C, Campbell PGC (2000) Silver uptake by the green alga *Chlamydomonas reinhardtii* in relation to chemical speciation: influence of chloride. Environ Toxicol Chem 19:2769–2778

Franklin NM, Rogers NJ, Apte SC, Batley GE, Gadd GE, Casey PS (2007) Comparative toxicity of nanoparticulate ZnO, bulk ZnO, and ZnCl2 to a freshwater microalga (Pseudokirchneriella sub-capitata): the importance of particle solubility. Environ Sci Technol 41:8484–8490. doi:10.1021/es071445r

Garcia-Cambero JP et al (2013) Converging hazard assessment of gold nanoparticles to aquatic organisms. Chemosphere 93:1194–1200. doi:10.1016/j.chemosphere.2013.06.074

Handy R et al (2012) Practical considerations for conducting ecotoxicity test methods with manufactured nanomaterials: what have we learnt so far? Ecotoxicology. doi:10.1007/s10646-012-0862-y

Hartmann NB, Von der Kammer F, Hofmann T, Baalousha M, Ottofuelling S, Baun A (2009) Algal testing of titanium dioxide nanoparticles—testing considerations, inhibitory effects and modification of cadmium bioavailability. Toxicology 269:190–197

Hartmann NB, Engelbrekt C, Zhang JD, Ulstrup J, Kusk KO, Baun A (2013) The challenges of testing metal and metal oxide nanoparticles in algal bioassays: titanium dioxide and gold nanoparticles as case studies. Nanotoxicology 7:1082–1094. doi:10.3109/17435390.2012.710657

Kahru A, Ivask A (2013) Mapping the dawn of nanoecotoxicological research. Acc Chem Res 46:823–833. doi:10.1021/ar3000212

Leclerc S, Wilkinson KJ (2014) Bioaccumulation of nanosilver by *Chlamydomonas reinhardtii*—nanoparticle or the free ion? Environ Sci Technol 48:358–364. doi:10.1021/es404037z

Le Faucheur S, Behra R, Sigg L (2005) Phytochelatin induction, cadmium accumulation, and algal sensitivity to free cadmium ion in Scenedesmus vacuolatus. Environ Toxicol Chem 24:1731–1737

Ma HB, Williams PL, Diamond SA (2013) Ecotoxicity of manufactured ZnO nanoparticles—a review. Environ Pollut 172:76–85. doi:10.1016/j.envpol.2012.08.011

Macfie SM, Tarmohamed Y, Welbourn PM (1994) Effects of cadmium, cobalt and nickel on growth of the green algae *Chlamydomonas reinhardtii*—the influence of the cell wall and pH. Arch Environ Contam Toxicol 27:454–458

Miao AJ, Schwehr KA, Xu C, Zhang SJ, Luo ZP, Quigg A, Santschi PH (2009) The algal toxicity of silver engineered nanoparticles and detoxification by exopolymeric substances. Environ Pollut 157:3034–3041. doi:10.1016/j.envpol.2009.05.047

Nam SH, Lee WM, Shin YJ, Yoon SJ, Kim SW, Kwak JI, An YJ (2014) Derivation of guideline values for gold(III) ion toxicity limits to protect aquatic ecosystems. Water Res 48:126–136. doi:10.1016/j.watres.2013.09.019

Navarro E, Baun A, Behra R, Hartmann NB, Filser J, Miao AJ, Quigg A, Santschi PH, Sigg L (2008a) Environmental behavior and ecotoxicity of engineered nanoparticles to algae, plants, and fungi. Ecotoxicology 17:372–386

Navarro E (2008b) Toxicity of silver nanoparticles to *Chlamydomonas reinhardtii*. Environ Sci Technol 42:8959–8964

Perreault F, Bogdan N, Morin M, Claverie J, Popovic R (2012) Interaction of gold nanoglycodendrimers with algal cells (*Chlamydomonas reinhardtii*) and their effect on physiological processes. Nanotoxicology 6:109–120. doi:10.3109/17435390.2011.562325

Piccapietra F, Allue CG, Sigg L, Behra R (2012a) Intracellular silver accumulation in *Chlamydomonas reinhardtii* upon exposure to carbonate coated silver nanoparticles and silver nitrate. Environ Sci Technol 46:7390–7397. doi:10.1021/es300734m

Piccapietra F, Sigg L, Behra R (2012b) Colloidal stability of carbonate-coated silver nanoparticles in synthetic and natural freshwater. Environ Sci Technol 46:818–825. doi:10.1021/es202843h

Pillai S, Behra R, Nestler H, Suter MJF, Sigg L, Schirmer K (2014) Linking toxicity and adaptive responses across the transcriptome, proteome, and phenotype of *Chlamydomonas reinhardtii* exposed to silver. Proc Natl Acad Sci USA 111:3490–3495. doi:10.1073/pnas.1319388111

Quigg A, Chin W-C, Chen C-S, Zhang S, Jiang Y, Miao A-J, Schwehr KA, Xu C, Santschi PH (2013) Direct and indirect toxic effects of engineered nanoparticles on algae: role of natural organic matter. Acs Sustain Chem Eng 1:686–702. doi:10.1021/sc400103x

Renault S, Baudrimont M, Mesmer-Dudons N, Gonzalez P, Mornet S, Brisson A (2008) Impacts of gold nanoparticle exposure on two freshwater species: a phytoplanktonic alga (*Scenedesmus subspicatus*) and a benthic bivalve (*Corbicula fluminea*). Gold Bull 41:116–126

Röhder LA, Brandt T, Sigg L, Behra R (2014) Influence of agglomeration of cerium oxide nanoparticles and speciation of cerium(III) on short term effects to the green algae *Chlamydomonas reinhardtii*. Aquat Toxicol 152:121–130. doi:10.1016/j.aquatox.2014.03.027

Scheidegger C, Sigg L, Behra R (2011) Characterization of lead induced metal-phytochelatin complexes in *Chlamydomonas reinhardtii*. Environ Toxicol Chem 30:2546–2552

Schirmer K, Behra R, Sigg L, Suter MJ-F (2013) Ecotoxicological aspects of nanomaterials in the aquatic environment. In: Luther W, Zweck A (eds) Safety aspects of engineered nanomaterials. Pan Stanford Publishing Pte. Ltd., Singapore, pp 141–162

Schreiber U (1998) Chlorophyll fluorescence: new instruments for special applications. Photosynth Mech Eff V:4253–4258

Segets D, Marczak R, Schafer S, Paula C, Gnichwitz JF, Hirsch A, Peukert W (2011) Experimental and theoretical studies of the colloidal stability of nanoparticles—a general interpretation based on stability maps. Acs Nano 5:4658–4669. doi:10.1021/nn200465b

Sigg L, Behra R, Groh K, Isaacson C, Odzak N, Piccapietra F, Röhder L, Schug H, Yue Y, Schirmer K (2014) Chemical aspects of nanoparticle ecotoxicology. Chimia 68:806–811. doi:10.2533/chimia.2014.806

Szivak I, Behra R, Sigg L (2009) Metal-induced reactive oxygen species production in *Chlamydomonas reinhardtii* (Chlorophyceae). J Phycol 45:427–435

Tai P, Zhao Q, Su D, Li P, Stagnitti F (2010) Biological toxicity of lanthanide elements on algae. Chemosphere 80:1031–1035. doi:10.1016/j.chemosphere.2010.05.030

Tsoli M, Kuhn H, Brandau W, Esche H, Schmid G (2005) Cellular uptake and toxicity of AU(55) clusters. Small 1:841–844. doi:10.1002/smll.200500104

Van Hoecke K, Quik JTK, Mankiewicz-Boczek J, De Schamphelaere KAC, Elsaesser A, Van der Meeren P, Barnes C, McKerr G, Howard CV, Van de Meent D, Rydzynski K, Dawson KA, Salvati A, Lesniak A, Lynch I, Silversmit G, De Samber B, Vincze L, Janssen CR (2009) Fate and effects of CeO2 nanoparticles in aquatic ecotoxicity tests. Environ Sci Technol 43:4537–4546

Van Hoecke K, De Schamphelaere KAC, Ali Z, Zhang F, Elsaesser A, Rivera-Gil P, Parak WJ, Smagghe G, Howard CV, Janssen CR (2013) Ecotoxicity and uptake of polymer coated gold nanoparticles. Nanotoxicology 7:37–47. doi:10.3109/17435390.2011.626566